Supplemental material

Savich et al., https://doi.org/10.1085/jgp.201812210

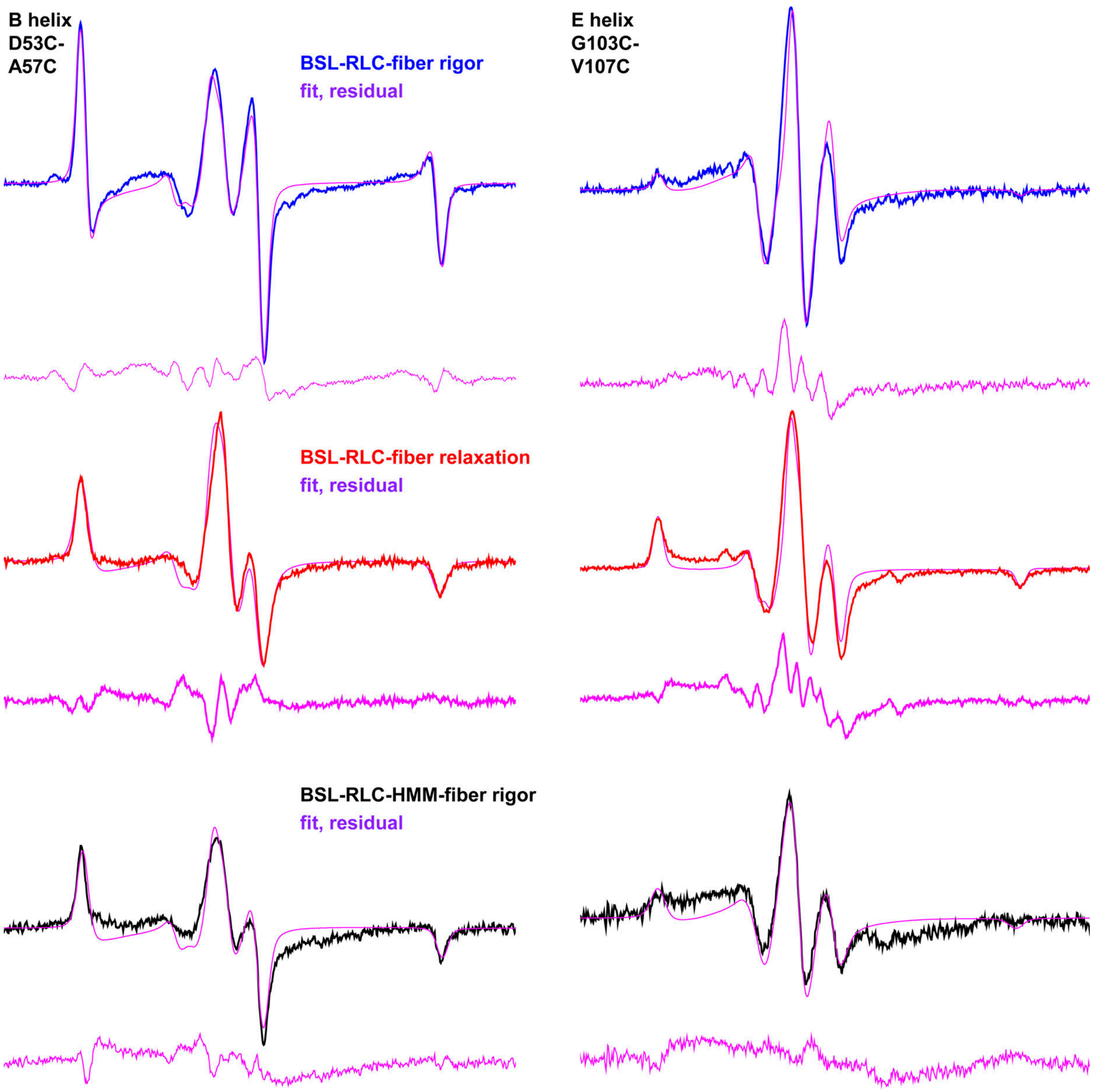

Figure S1. **EPR data on BSL-RLC-fiber in rigor (blue), BSL-RLC-fiber in relaxation (red), and BSL-RLC-HMM-fiber in rigor (black).** Fits and residuals are in magenta. Static limit was assumed during fitting. The field sweep width shown is 100 G.

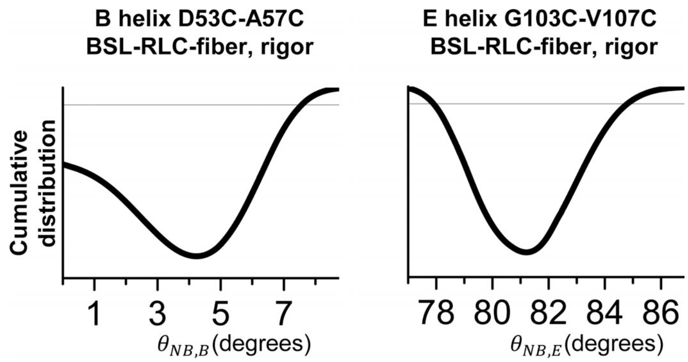

Figure S2. **The cumulative distribution function of the F-ratio distribution, comparing the ratio of the residual sum of squares of the fits with the residual sum of squares of the best fit.** The 95% intervals are depicted by horizontal lines. The confidence interval for helix B is flatter on the left-hand side, as compared with helix E. This happens due to the vanishing of the derivatives of the g and A tensors (Eqs. S2 and S3) $\frac{\partial g}{\partial \theta_{NB}}$ and $\frac{\partial A}{\partial \theta_{NB}}$ at the turning points ($\theta_{NB} = 0^\circ, 90^\circ$). Since those tensors define the spectral position of a given probe orientation (Eq. S1), the EPR spectrum is not sensitive to orientation near the turning points. However, the symmetry of the resonance position $B_{res}(-\theta_{NB}) = B_{res}(\theta_{NB})$ restricts $\theta_{NB} > 0^\circ$ for the B helix, which brings the angular resolution for the probes on both helices to 4°.

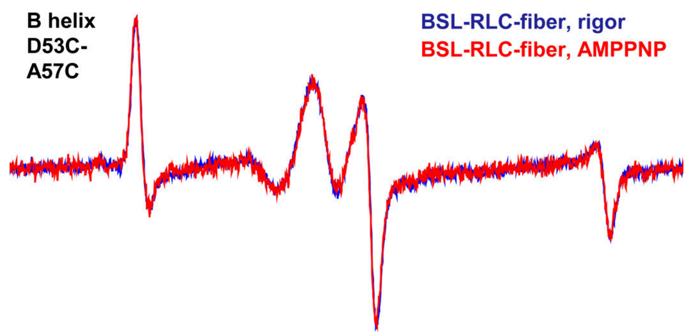

Figure S3. **The effect of 5 mM AMPPMP (red) on a BSL–RLC–fiber labeled on the B helix in rigor (blue) during EPR.** The field sweep width is 100 G.

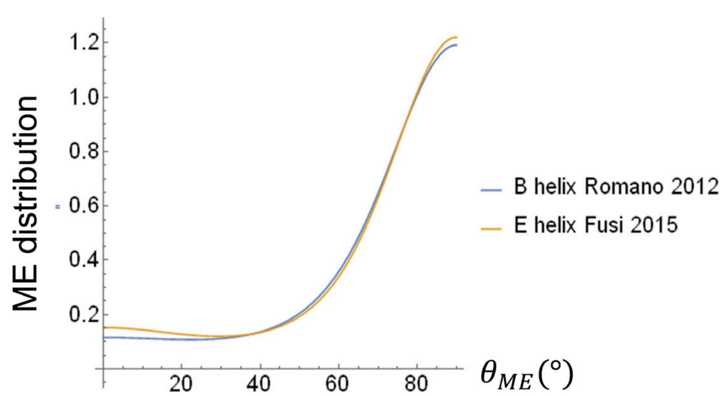

Figure S4. **The ME distributions (calculated according to Eqs. S4–S7) for the B and E helix calculated from reported order in fluorescence polarization experiments.** The B and helix E orienting potentials (reproduced here from digitized figures using GetData GraphDigitizer, v.2.26) are $-0.296\,P_2(\cos\alpha) + 0.118\,P_4(\cos\alpha)$ (Romano et al., 2012) and $-0.293\,P_2(\cos\alpha) + 0.127\,P_4(\cos\alpha)$ (Fusi et al., 2015), respectively, where α is the angle between the BR dipole and the muscle fiber, $p_n(x)$ is the nth order Legendre polynomial, and the coefficients are the respective order parameters. Since $P_2(\cos\alpha)$ varies from 1 to −0.5 as α goes from 0° to 90°, and $P_2(\cos\alpha)$ varies from +1 to −0.43 as α goes from 0° to 50°; such a small difference in the order parameters between the B and E helices yields indistinguishable ME distributions.

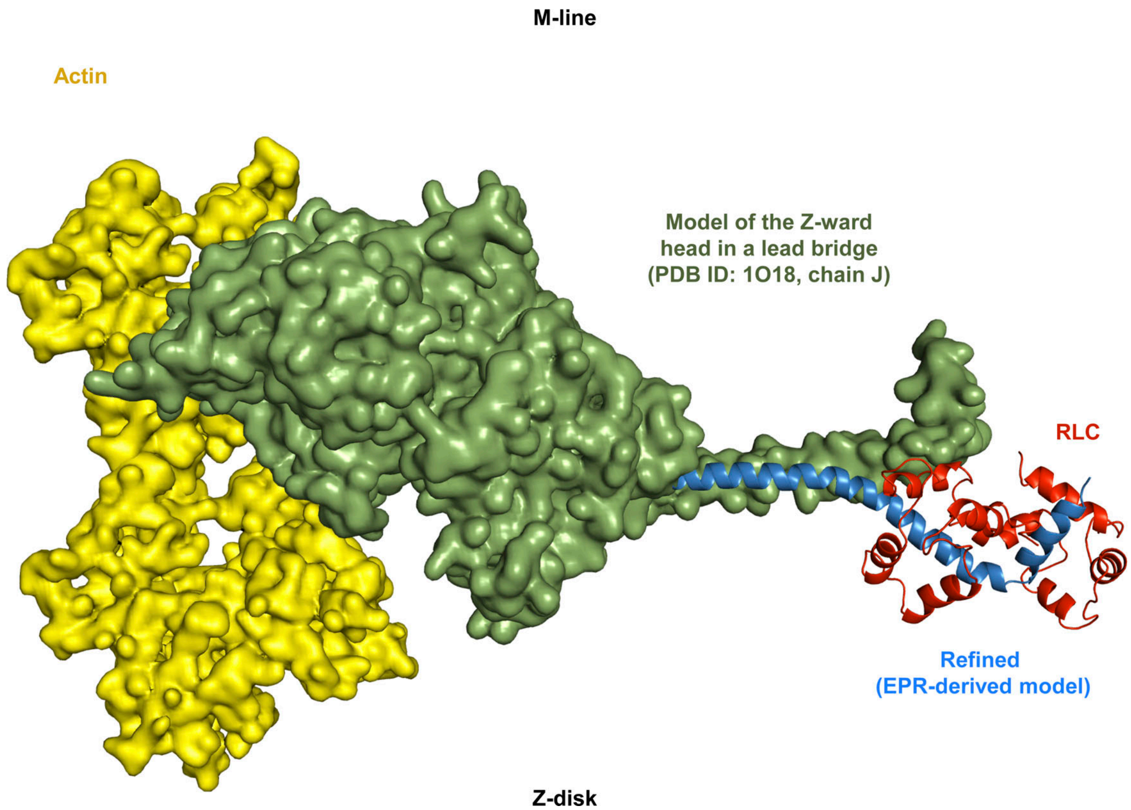

Figure S5. **Alignment of the EPR-derived model (blue lever arm helix, red RLC) with the Z-ward head (green) of the lead bridge in the 7-nm-resolution model derived from insect flight muscle tomography.** From PDB accession number 1O18, chain J (Chen et al., 2002). Actin is shown in yellow and RLC in red. The alignment was done via the lower 50-kD domain.

Table S1. **Fitting parameters of the oriented fiber experiments**

	θ_{NB}(°)	σ(°)	Mole fraction
B helix (53–57)			
RLC–fiber rigor (first component)	4 ± 4	9 ± 3	0.11 ± 0.02
RLC–fiber rigor (second component)	22 ± 15	>38	0.89 ± 0.02
RLC–fiber relaxation (single component)	18 ± 14	>38	—
RLC–HMM–fiber rigor (single component)	32 ± 14	>38	—
E helix (103–107)			
RLC–fiber rigor (first component)	81 ± 4	11 ± 3	0.54 ± 0.03
RLC–fiber (second component)	86 ± 18	>38	0.46 ± 0.03
RLC–fiber relaxation (single component)	51 ± 15	>38	—
RLC–HMM–fiber rigor (first component)	81 ± 4	11 ± 3	0.25 ± 0.03
RLC–HMM–fiber rigor (second component)	88 ± 16	>38	0.75 ± 0.03

Errors are propagated from 95% confidence intervals imposed on the simulated fit error surface.

EPR equations

The position of resonance in an EPR experiment at a given orientation θ_{NB}, ϕ_{NB} of a spin label π orbital is given by

$$B_{res} = \frac{h\nu}{\mu_B g(\theta_{NB}, \phi_{NB})} - m_I A(\theta_{NB}, \phi_{NB}), \quad \text{(S1)}$$

where h is the Planck constant, ν is the microwave frequency, μ_B is the Bohr magneton, m_I is the N^{14} nuclear quantum number (−1, 0, 1), $g(\theta_{NB},\phi_{NB})$, and $A(\theta_{NB}, \phi_{NB})$ are Zeeman and hyperfine tensors whose eigenvalues determine anisotropy of the system:

$$g^2(\theta_{NB}, \phi_{NB}) = g_x^2 \sin^2\theta_{NB} \cos^2\phi_{NB} + g_x^2 \sin^2\theta_{NB} \sin^2\phi_{NB} + g_z^2 \cos^2\theta_{NB}, \quad \text{(S2)}$$

and

$$A^2(\theta_{NB}, \phi_{NB}) = A_x^2 \sin^2\theta_{NB} \cos^2\phi_{NB} + A_x^2 \sin^2\theta_{NB} \sin^2\phi_{NB} + A_z^2 \cos^2\theta_{NB}. \quad \text{(S3)}$$

ME equations

Once $\langle P_2(\cos\alpha)\rangle$ and $\langle P_4(\cos\alpha)\rangle$ are obtained in an experiment, there is a continuum of orientational distribution functions that yield $\langle P_2(\cos\alpha)\rangle$ and $\langle P_4(\cos\alpha)\rangle$. The ME distribution function maximizes informational entropy and thus yields the broadest distribution that serves as a low-resolution approximation of the angular distribution of the probe. The ME distribution is defined as

$$f(a, \lambda_2, \lambda_4) = Z(\lambda_2, \lambda_4)^{-1} \exp[-\lambda_2 P_2(\cos\alpha) - \lambda_4 P_4(\cos\alpha)], \quad \text{(S4)}$$

where λ_2, λ_4 are Lagrange multipliers and $Z(\lambda_2, \lambda_4)$ is a normalization factor:

$$Z(\lambda_2, \lambda_4) = \int_0^\pi d\alpha \, \exp[-\lambda_2 P_2(\cos\alpha) - \lambda_4 P_4(\cos\alpha)] \sin\alpha. \quad \text{(S5)}$$

We determine λ_2, λ_4 by

$$\langle P_2(\cos\alpha)\rangle = \int_0^\pi d\alpha \, P_2(\cos\alpha) \, f(a, \lambda_2, \lambda_4) \sin\alpha, \quad \text{(S6)}$$

and

$$\langle P_4(\cos\alpha)\rangle = \int_0^\pi d\alpha \, P_4(\cos\alpha) \, f(a, \lambda_2, \lambda_4) \sin\alpha. \quad \text{(S7)}$$

References

Chen, L.F., H. Winkler, M.K. Reedy, M.C. Reedy, and K.A. Taylor. 2002. Molecular modeling of averaged rigor crossbridges from tomograms of insect flight muscle. *J. Struct. Biol.* 138:92–104. https://doi.org/10.1016/S1047-8477(02)00013-8

Fusi, L., Z. Huang, and M. Irving. 2015. The Conformation of Myosin Heads in Relaxed Skeletal Muscle: Implications for Myosin-Based Regulation. *Biophys. J.* 109:783–792. https://doi.org/10.1016/j.bpj.2015.06.038

Romano, D., B.D. Brandmeier, Y.B. Sun, D.R. Trentham, and M. Irving. 2012. Orientation of the N-terminal lobe of the myosin regulatory light chain in skeletal muscle fibers. *Biophys. J.* 102:1418–1426. https://doi.org/10.1016/j.bpj.2012.02.010